Electron Transfer Reactions. A Reinvestigation of the Chlorination of 1-Methyl-2-phenylindole with *N*-Chlorobenzotriazole. The Role of Oxygen and Oxygenated Solvent

Patricia Carloni,[a] Lennart Eberson,*[,b] Lucedio Greci,*[,a] Pierluigi Stipa[a] and Giorgio Tosi[a]
[a] *Dipartimento di Scienze dei Materiali e della Terra, Università di Ancona, Via Brecce Bianche, I-60131 Ancona, Italy*
[b] *Organic Chemistry 3, Chemical Center, University of Lund, PO Box 124, S-22100 Lund, Sweden*

1-Methyl-2-phenylindole (**1**, MPI-H) reacts with *N*-chlorobenzotriazole (**2**, BT-Cl) to form the corresponding radical cation $(\text{MPI-H})^{\cdot+}$ which itself, or *via* the indolyl radical $(\text{MPI})^{\cdot+}$, formed by deprotonation of $\text{MPI-H}^{\cdot+}$, reacts with oxygen or a nucleophilic solvent leading to indoxyls **4**–**7**. Cyclic voltammetric studies, as well as the oxidation of MPI-H with BT-Cl carried out in the EPR cavity, show that the radical cation $\text{MPI-H}^{\cdot+}$ dimerizes to give $3,3'\text{-(MPI)}_2$ **8** which is transformed into the corresponding radical cation $3,3'\text{-(MPI)}_2^{\cdot+}$ in the reaction medium. The identity of this radical cation has been confirmed by oxidizing $3,3'\text{-(MPI)}_2$ directly. The formation of the radical cations $\text{MPI-H}^{\cdot+}$ and $3,3'\text{-(MPI)}_2^{\cdot+}$ has been monitored by UV–VIS spectroscopy and their decay rate constants measured.

Some years ago we described the reaction between 1-methyl-2-phenylindole (**1**, MPI-H) and *N*-chlorobenzotriazole (**2**, BT-Cl),[1] and the reaction mechanism was suggested to involve formation of the indole radical cation in an initial electron transfer (ET) step between the reactants as in eqn. (1).

$$1 + \text{BT-Cl} \longrightarrow 1^{\cdot+} + \text{BT}^{\cdot} + \text{Cl}^{-} \qquad (1)$$

This mechanism explained the formation of indoxyls **4**–**7** (Scheme 1) as being due to interaction between various indole radical cations and adventitious water in the medium.[2,3]

However, since the amount of water required for these nucleophilic reactions exceeded any reasonable estimate of how much could actually be present, we have undertaken a reinvestigation of the reaction. This study confirms that the indole radical cation is an intermediate and that the formation of indoxyls is due to the presence of dioxygen and oxygenated nucleophiles in the reaction medium.

Results and Discussion

The reaction of 1-methyl-2-phenylindole (MPI-H, the H belonging to position 3 of the indole nucleus) with BT-Cl was carried out at room temperature in a non-nucleophilic solvent under nitrogen, argon or air with ultrasound, or in a nucleophilic solvent such as acetic acid. In a deoxygenated, dry non-nucleophilic solvent the product was ⩾90% 3-Cl-MPI (**3**) with minor amounts of indoxyls **4** and **5**, whereas under identical conditions but with air present, the yield of 3-Cl-MPI decreased to 30–40% with a concomitant increase in the yield of indoxyls (sum *ca.* 40%). Addition of *ca.* 3% acetic acid to benzene under a nitrogen atmosphere increased the yield of **4** + **5** at the expense of 3-Cl-MPI and this tendency became even more pronounced in 100% acetic acid/N_2. Addition of sodium acetate (0.1 mol dm^{-3}) had no significant effect under the latter set of conditions (Table 1).

These experiments suggest that dioxygen must be involved in the side reactions of $\text{MPI-H}^{\cdot+}$, formed in an ET step between BT-Cl and MPI-H. Evidence for this assumption was obtained by the UV–VIS and EPR spectroscopic and voltammetric experiments described below.

Trifluoroacetic acid (TFA) is known to stabilize radical cations and we therefore conducted rapid-mixing experiments of solutions of MPI-H (23 mmol dm^{-3}) and BT-Cl (26 mmol dm^{-3}) in dichloromethane–TFA (80/20 v/v) and monitored them by UV–VIS spectroscopy. Fig. 1 shows a series of spectra, taken at 2 s intervals, showing the very rapid appearance of a

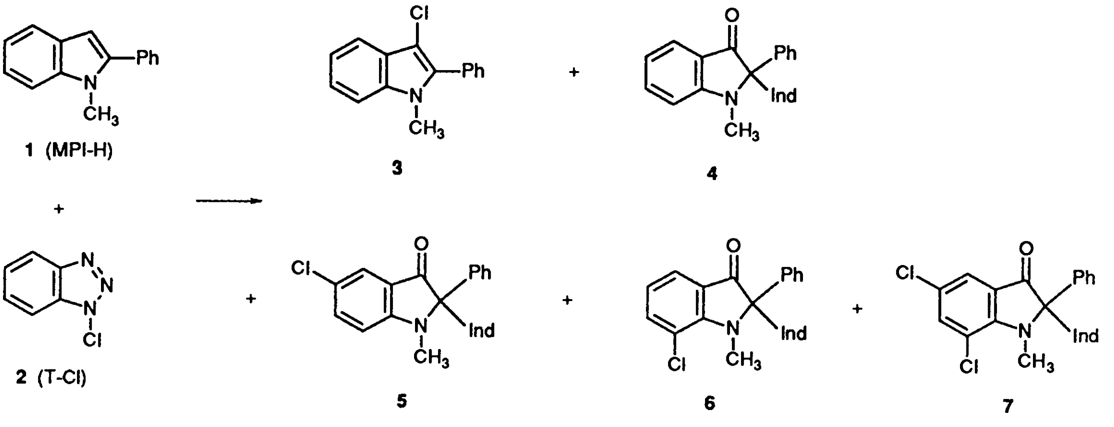

Ind = 1-methyl-2-phenylindol-3-yl
Scheme 1

Table 1 Product distribution from the reaction between MPI-H and BT-Cl under various conditions, at room temperature.

Conditions	Recovered MPI-H (%)	Yield of product (%)[a] 3	4	5	6 + 7
Benzene/N_2	0	90	4	6	0
Benzene/Ar[b]	0	100	0	0	0
Benzene/air	31	32	14	7	16
Dichloromethane/N_2	3	95	2	0	0
Dichloromethane/air	12	43	35	8	2
Benzene/AcOH/N_2	2	79	14	5	0
AcOH/N_2	23	38	12	15	12
AcOH/NaOAc/N_2	13	41	19	13	14

[a] The reported yields are the ratio of the identified products evaluated by HPLC; the material balance was in each case over 95%. [b] With ultrasound treatment.

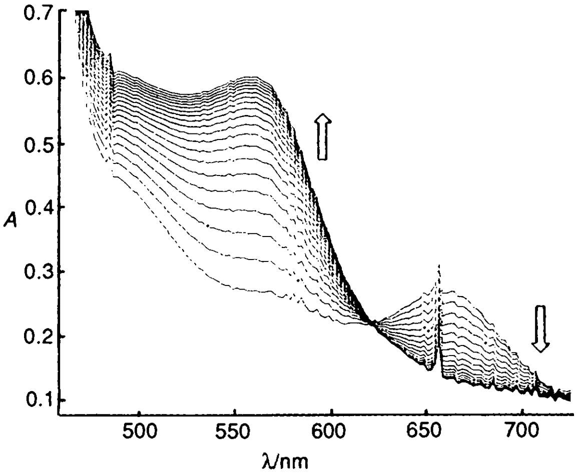

Fig. 1 Spectra, taken at 2 s intervals, of a solution initially 11.5 mmol dm^{-3} in MPI-H and 13 mmol dm^{-3} in BT-Cl in dichloromethane–TFA (80/20 v/v) at 23 °C

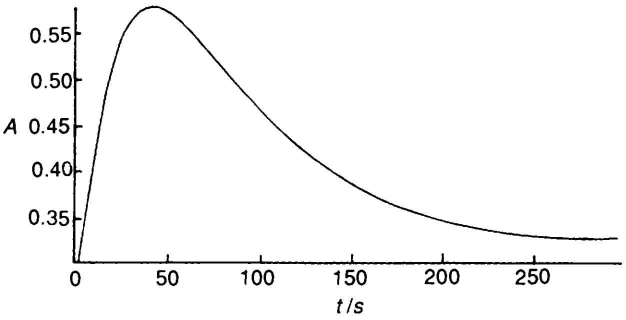

Fig. 2 Monitoring the absorbance at 558 nm from a solution initially 5.0 mmol dm^{-3} in MPI-H and 8.5 mmol dm^{-3} in BT-Cl in dichloromethane–AcOH (95:5 v/v) at 23 °C

band at λ_{max} 662 nm which we ascribe to $MPI\text{-}H^{\bullet +}$; this species decays with a rate constant of *ca.* 7 min^{-1} at ambient temperature.

The *N*-chlorobenzotriazole (BT-Cl) is not affected by trifluoroacetic acid even if a protonation equilibrium is present; however, we believe that the electron transfer mechanism is still operating in the same way as described above.

At the same time, a band with λ_{max} 558 nm appears at an approximately equal rate. The latter absorption is assigned to the dehydrodimer radical cation of MPI-H, 3,3′-$(MPI)_2^{\bullet +}$ ($\mathbf{8}^{\bullet +}$). In a similar experiment, using dichloromethane containing the stronger nucleophile, acetic acid (5% v/v), but with lower initial [MPI-H] and [BT-Cl] of 5.0 and 8.5 mmol dm^{-3}, respectively, only the dynamics of the 558 nm band could be observed whereas the 662 nm band was not detectable. Fig. 2 shows the biphasic kinetic behaviour of $(MPI)_2^{\bullet +}$ under these conditions; it is formed with a rate constant of *ca.* 3 min^{-1} and decays with rate constant of *ca.* 0.8 min^{-1} at 20 °C. Its lack of stability in dichloromethane–AcOH is of course due to the higher nucleophilicity of acetic acid as compared to that of TFA.

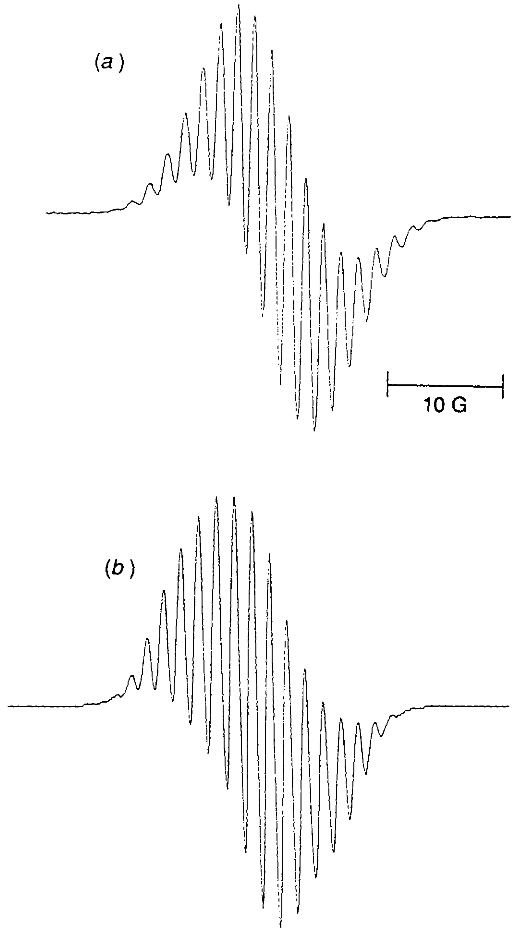

Fig. 3 EPR spectrum of a solution resulting from 48 mmol dm^{-3} of MPI-H and 78 mmol dm^{-3} of BT-Cl in 95:5 dichloromethane–AcOH recorded at room temperature: (*a*) experimental, (*b*) computer simulated with 10 H (1.38 G), 2 N (3.1 G), line width = 0.9 G

Mixing and degassing (Ar) solutions of MPI-H (48 mmol dm^{-3}) and BT-Cl (78 mmol dm^{-3}) in 95/5 dichloromethane–AcOH produced a solution which initially displayed an intense, unresolved EPR signal. It gradually changed over *ca.* 15 min into a 19-line signal (Fig. 3*a*) with $g = 2.0027$. This spectrum was simulated on the basis of the spin density distribution reported in Table 2 for a model compound, and of hf.c.c.s reported in the caption to Fig. 3* (Fig. 3*b*).

The same signal was obtained when a few crystals of BT-Cl were added to the top of a frozen, deoxygenated solution of MPI-H in dichloromethane with a trace of TFA added, and the tube allowed to reach room temperature in the EPR cavity. Authentic 3,3′$(MPI)_2$ (**8**) upon treatment with BT-Cl under the same conditions as given above, or upon oxidation with tris(4-bromophenyl)aminium hexachloroantimonate (**9**), again produced the same signal.

In connection with the electrochemical studies it was noticed

---

* Hyperfine coupling constants reported in Fig. 3 even reproducing quite well the experimental signal are indicative because of the spectral shape and the high value of the line width used in the simulation. This set of hf.c.cs is in agreement with the spin density distribution reported in Table 2.

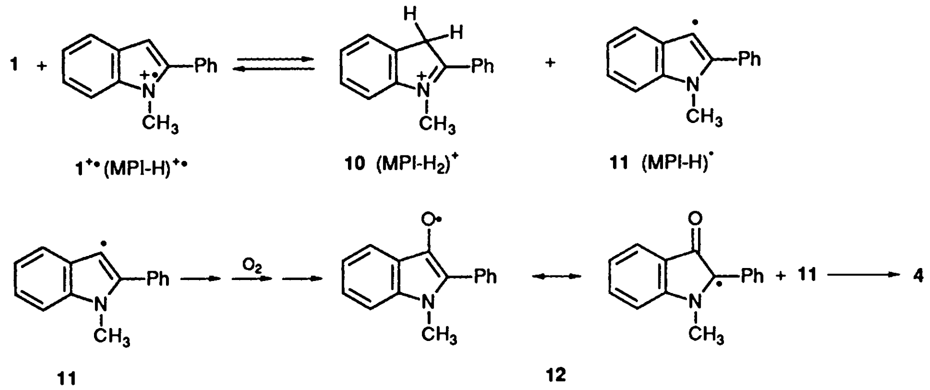

Scheme 2

Table 2 Spin density distributions

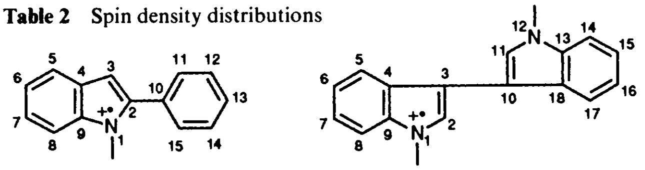

Position	McLachlan spin density	Position	McLachlan spin density
1	0.0388	1	0.0260
2	0.1780	2	0.2489
3	0.4234	3	0.1466
4	−0.0579	4	−0.0165
5	0.1587	5	0.0447
6	−0.0464	6	−0.0098
7	0.1119	7	0.0351
8	0.0160	8	0.0013
9	0.0544	9	0.0236
10	−0.0095	10	0.1466
11	0.0599	11	0.2489
12	−0.0257	12	0.0260
13	−0.0643	13	0.0236
14	−0.0257	14	0.0013
15	0.0599	15	0.0351
		16	−0.0098
		17	0.4470
		18	0.0165

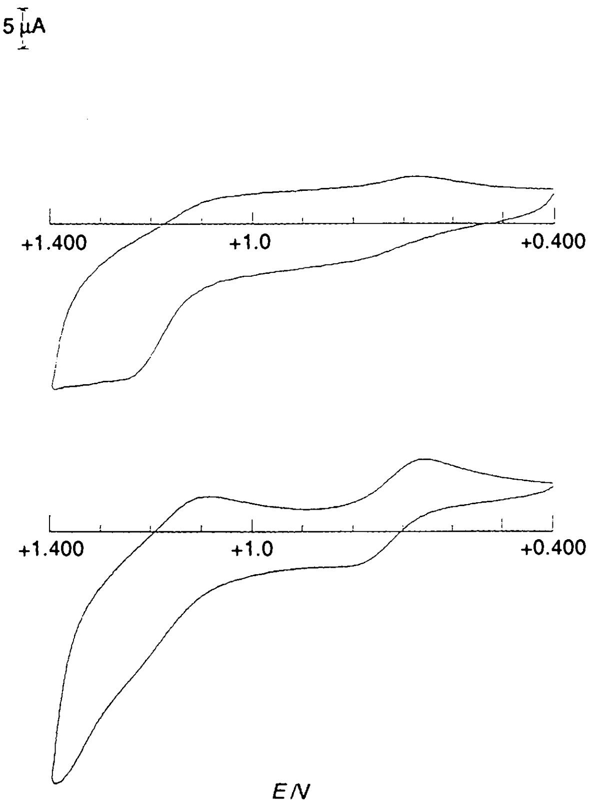

Fig. 4 Cyclic voltammograms of 1 mmol dm^{-3} solutions of MPI-H (upper curve) and 3,3′-(MPI)$_2$ (lower curve) under argon in dichloromethane–tetrabutylammonium hexafluorophosphate (0.1 mol dm^{-3}) at sweep rate of 2000 mV s^{-1}

that an Ar degassed solution of 3,3′-(MPI)$_2$ in dichloromethane–TFA–TFA anhydride (80/15/5) gave weak signal due to **8**$^{\bullet +}$, whose amplitude was enhanced by a factor of *ca.* seven by bubbling oxygen through the solution for 30 s followed by renewed Ar degassing (3 min). An additional O$_2$ bubbling (4 min)/Ar degassing (3 min) sequence increased the amplitude of the EPR signal by another factor of three. The same EPR signal was also detectable in solutions of MPI-H or 3,3′-(MPI)$_2$ in dichloromethane after exposure to air.

Cyclic voltammetry of MPI-H in a non-nucleophilic medium, dichloromethane–tetrabutylammonium hexafluorophosphate (0.1 mol dm^{-3}), displayed an irreversible oxidation wave with E_{pa} *ca.* 1.25 V (Ag/AgCl). Prolonged cycling showed the development of two reversible couples corresponding to those of 3,3′-(MPI)$_2$ (Fig. 4, run under argon at a sweep rate of 2000 mV s^{-1}). At lower sweep rates (100–200 mV s^{-1}), the two new couples were less easily discernible. When oxygen was admitted to the solution at low sweep rate, the 3,3′-(MPI)$_2$ couples disappeared; they were restored after renewed Ar degassing. A facile reaction with oxygen was noted upon dissolution of both MPI-H and 3,3′-(MPI)$_2$ in dichloromethane, in that a green-brown colouration developed after only a few seconds. These solutions were EPR-active, showing the same spectrum as described above.

In the more nucleophilic medium, dichloromethane–acetic acid (90/10)–tetrabutylammonium hexafluorophosphate (0.1 mol dm^{-3}) no colouration developed and the cyclic voltammogram displayed quantitatively the same behaviour as above, with well developed secondary couples centered at 0.73 and 1.09 V due to 3,3′-(MPI)$_2$. No oxygen effect was seen even at low sweep rates.

In another nucleophilic medium, acetonitrile–tetrabutylammonium hexafluorophosphate (0.1 mol dm^{-3}), again no colouration developed. At 500 mV s^{-1}, the cyclic voltammogram (Fig. 5) had a similar appearance as that in dichloromethane, except for the fact that the two waves due to 3,3′-(MPI)$_2$ were lower as compared to the MPI-H oxidation wave. Oxygen had no effect on the cyclic voltammogram under these conditions. 3,3′-(MPI)$_2$ (**8**) gave almost reversible behaviour in this medium (at 100 mV s^{-1}, $E_{rev}{}^1$ = 0.74 V with peak separation = 69 mV and $E_{rev}{}^2$ = 1.04 V with peak separation = 61 mV).

The kinetic experiments described above further indicate that BT-Cl reacts with MPI-H in an initial ET step [eqn. (1)]. In a

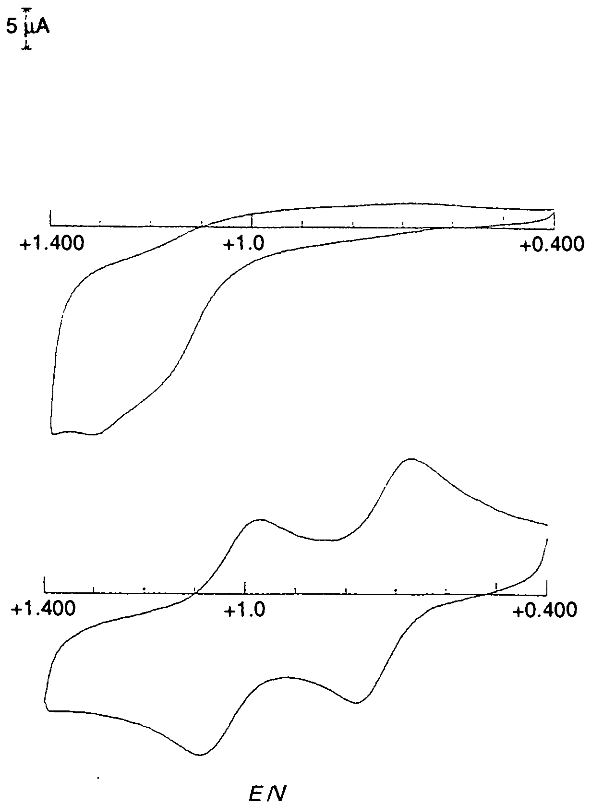

Fig. 5 Cyclic voltammograms of a 1 mmol dm^{-3} solution of MPI-H (upper curve) and a saturated solution of 3,3'-(MPI)$_2$ (lower curve) in acetonitrile–tetrabutylammonium hexafluorophosphate (0.1 mol dm^{-3}) at sweep rate of 500 mV s^{-1}

non-nucleophilic solvent (dichloromethane–TFA) one can actually detect a very fast development of MPI-H$^{\cdot+}$ (Fig. 1), followed by its disappearance (rate constant *ca.* 7 min^{-1}) due to formation of the dimer radical cation, 3,3'-(MPI)$_2$. The latter is also detectable in dichloromethane–AcOH (Fig. 2). Also, EPR and CV experiments show that 3,3'-(MPI)$_2^{\cdot+}$ is formed upon ET oxidation of MPI-H which raises the question of the role of this type of dimeric species in the overall reaction. No dimeric products are derived from the 3,3'-structure (Scheme 1) and since the material balances are good (Table 1), there must be a reason for its disappearance. We suggest that 3,3'-(MPI)$_2$ simply acts as supply of MPI-H$^{\cdot+}$ for eventual capture by chloride ion [eqns. (2) and (3)] or another nucleophile.

$$2\text{MPI-H}^{\cdot+} \rightleftharpoons (\text{H-MPI-MPI-H})^{2+} \rightleftharpoons 3,3'\text{-(MPI)}_2 + 2\text{H}^+ \quad (2)$$

$$\text{MPI-H}^{\cdot+} + \text{Cl}^- \longrightarrow \text{MPI(Cl)H}^{\cdot} \xrightarrow{-e^-} \text{MPI(Cl)H}^+ \longrightarrow \text{MPIHCl} + \text{H}^+ \quad (3)$$

As to the mechanism for the formation of indoxyl **4**, two hypotheses could be advanced. The first is through a reversible protonation of **1** by the radical cation **1**$^{\cdot+}$ forming the indolyl radical **11**, according to the literature reports,[4] (Scheme 2), which, by reacting with oxygen[5] could eventually lead to the indolyloxy radical **12**. The latter could form indoxyl **4** by coupling with an indolyl radical **11** (Scheme 2).

The second possible mechanism for the formation of indoxyls **4** involves an interaction between MPI-H$^{\cdot+}$ and dioxygen. This assumption should be supported by the pK_a of MPI-H$^{\cdot+}$ which is 11.96 [calculated from a literature report[6] assuming ΔG°(BDE) of the C(3)-H = 70 kcal mol^{-1}], too high to allow an easy deprotonation as previously described. Although the attack of dioxygen on MPI-H$^{\cdot+}$ is disfavoured owing to its low electrophilic character, the oxygen attack could be possible on the basis of the high spin density on C(3), as it can be deduced from Table 2.

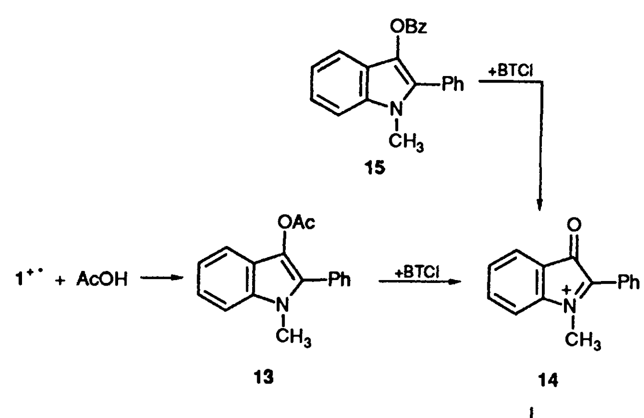

Scheme 3

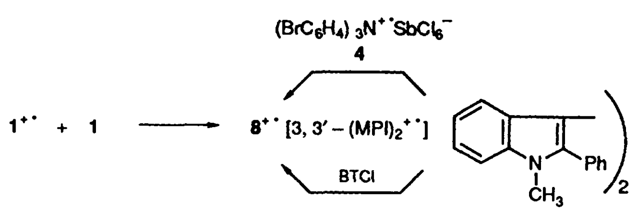

8 [3,3'-(MPI)$_2$]

As for the reaction with acetic acid, we suggest that Scheme 3 offers a plausible pathway to **4** which is in line with previous work.[7]

In further support of this proposal, the benzoyloxy derivative **15**, MPI-H and BT-Cl reacted in deoxygenated benzene in a 1:1:1 molar ratio to give indoxyls **4**–**7** in high yield, as expected considering their derivation from benzyloxy derivative **15**.

Experimental

Methods.—Cyclic voltammetry was performed with the BAS-100 instrument, using a platinum button working electrode, an Ag/AgCl reference electrode and a Pt wire as counter electrode. EPR spectra were run on Bruker ER 200D SRC and Varian E4 instruments. Kinetics were monitored by an HP 8452A spectrophotometer equipped with the HP 89500 UV–VIS ChemStation, fast experiments being performed in the stopped-flow accessory RX.1000 from Applied Photophysics Ltd., Leatherhead, England. Liquid chromatography was performed on a Perkin-Elmer series 2 HPLC (conditions: eluent = MeOH–H$_2$O (84:16); flow = 1.2 cm^3 min^{-1}; temperature = 55 °C; column = Nucleosil-R C-18 5μm).

Compounds **1**[8], **2**[9], **9**[10] and **15**[11] were prepared as described in the literature. The 3-Cl-MPI and indoxyls **4**–**7** were identified by comparison with authentic samples prepared as described in the literature.[1]

Reaction between 1-*Methyl*-2-*phenylindole* (**1**) *and* N-*Chlorobenzotriazole* (**2**).—A 2 mmol sample of indole in 25 cm^3 of solvent and 2 mmol of BT-Cl in 25 cm^3 of solvent were put separately into the two legs of an inverted Y flask, saturated with N$_2$, air or Ar, with ultrasound and then mixed at room temperature. After 3 h the reaction mixture was concentrated and analysed by HPLC.

Reaction of 1-*Methyl*-2-*phenylindole* (**1**) *with* N-*Chlorobenzotriazole* (**2**) *and* 1-*Methyl*-2-*phenyl*-3-*benzoyloxyindole* (**15**). A sample of 2 mmol of indole and 2 mmol of **15** in 25 cm^3 of deoxygenated benzene and a sample of 2 mmol of BT-Cl in 25 cm^3 of deoxygenated benzene were put separately into the two legs of an inverted Y flask and then mixed at room temperature. After 3 h the reaction mixture was concentrated and analysed by HPLC giving the following yields: **1** + **15** = 28%, **3** = 46%, **4** = 17%, **5** + **6** = 8% and **7** = 1%.

EPR Study.—EPR experiments were carried out using an inverted U cell, similar to that described in the literature.[12]

MacLachlan Spin Density Distribution.—The spin density distribution was calculated by a computer program[13] with the following values: $h_{N^{\cdot +}} = 1.85$; $K_{C\text{–}C} = 1.0$; $\lambda = 1.2$.

Acknowledgements

We thank the *Ministero della Università, della Ricerca Scientifica e Tecnologica* (*M.U.R.S.T.*), and the *C.N.R.* (*Progetto strategico: processi di trasferimento elettronico*), for financial support.

References

1 C. Berti, L. Greci, R. Andruzzi and A. Trazza, *J. Org. Chem.*, 1982, **47**, 4895.
2 A. J. Bard, A. Ledwith and H. J. Shine, *Adv. Phys. Org. Chem.*, 1976, **13**, 227.
3 A. H. Jackson and P. Smith, *J. Chem. Soc. C*, 1968, 1967.
4 (*a*) X. Shen, J. Lind and G. Merényi, *J. Phys. Chem.*, 1987, **91**, 4403; (*b*) X. Shen, J. Lind, T. E. Eriksen and G. Merényi, *J. Chem. Soc.. Perkin Trans. 2*, 1990, 597.
5 J. A. Howard, *Rev. Chem. Intermed*, 1984, **5**, 1.
6 A. Martin De P. Nicholas and D. R. Arnold, *Can. J. Chem.*, 1982, **60**, 2165.
7 S. Torii, T. Yamanaka and H. Tanaka, *J. Org. Chem.*, 1978, **43**, 2882.
8 M. Colonna, L. Greci and M. Poloni, *J. Chem. Soc.. Perkin Trans. 2*, 1980, 628.
9 C. W. Rees and R. C. Storr, *Chem. Commun.*, 1968, 1305.
10 F. A. Bell, A. Ledwith and D. C. Sherrington, *J. Chem. Soc. C*, 1969, 2719.
11 M. Colonna, L. Greci and M. Poloni, *Tetrahedron Lett.*, 1981, **22**, 1143.
12 G. A. Russell, E. G. Janzen and E. T. Strom, *J. Am. Chem. Soc.*, 1964, **86**, 1807.
13 A. D. MacLachlan, *Mol. Phys.*, 1960, **3**, 233.

Paper 1/03581I
Received 15th *July* 1991
Accepted 1st *August* 1991